Reappraisal of the crystal chemistry of beryl

C. Aurisicchio
Centro di Studio per la Mineralogia e Petrologia delle Formazioni Ignee, C.N.R., 00100 Roma, Italy

G. Fioravanti, O. Grubessi
Dipartimento di Scienze della Terra, Università "La Sapienza," 00100 Roma, Italy

P. F. Zanazzi*
Dipartimento di Scienze della Terra, Università di Perugia, 06100 Perugia, Italy

Abstract

The complex crystal chemistry of beryl has been re-evaluated on the basis of new chemical analyses and X-ray structural refinements on beryl samples of different sources and compositions.

The results show that main substitutions concern divalent and Li ions for Al in octahedral and Be in tetrahedral sites, respectively; both substitutions need the entry of alkali in the $2a$ position in the channels between the six-membered Si rings, whereas the $2b$ position at the center of each ring is occupied preferentially by water molecules. The extent of the substitutions for Al and Be is limited by the imbalance arising from the bond-strength deficiency on $O(2)$. The effect of these substitutions on the lattice parameters allows the definition of three beryl series on the basis of the c/a ratio: the "octahedral" beryls, i.e., beryls where $Al \rightleftharpoons Me^{2+}$ represents the main isomorphous replacement, are characterized by c/a values in the range 0.991–0.996; the "tetrahedral" beryls, where Be $\rightleftharpoons$ Li is the main substitution, with c/a values in the range 0.999–1.003; the "normal" beryls with c/a ratios between 0.997 and 0.998 include those where the two substitutions occur together, though to a limited extent. A compositional gap exists between "octahedral" and "tetrahedral" beryls. The formation of beryls of a given series has been ascribed to the chemical constraints of the environment, such as the bulk-rock chemistry and the fluid-phase composition, and to the physical-chemical conditions during mineral growth.

Introduction

Beryl, ideally $Al_2Be_3Si_6O_{18}$, is an accessory mineral found in many pegmatites, in silicic rocks of various geneses, as well as in mafic metamorphic rocks.

The structure of the mineral has long been known (Bragg and West, 1926; Gibbs et al., 1968). It consists of six-membered rings of Si tetrahedra lying in planes parallel to (0001). These rings are linked together both laterally and vertically by Be tetrahedra and Al octahedra forming a three-dimensional framework that, according to the silicate classification of Zoltai (1960), is to be considered as a tectosilicate. The structure contains channels parallel to the c axis where minor constituents such as alkali ions and water molecules can be located, as normally found in natural beryls. The presence of alkali ions is generally ascribed to the need to balance the deficiency of positive charges resulting from the replacement of octahedral Al and tetrahedral Be by cations of lower valence, such as Fe^{2+}, Mn^{2+}, Mg^{2+}, Li^+, etc. The mineral shows variations of physical properties because of a very complex crystal-chemical behavior. In spite of the numerous and

accurate papers on beryl crystal chemistry, some intriguing questions still persist: for example, it has not been clear whether beryl forms a continuous isomorphous series or two series with substitutions in the octahedral sites and tetrahedral sites, respectively (Schaller et al., 1962; Bakakin et al., 1970). While there is general agreement that divalent cations substitute for Al in octahedral sites and Li for Be in tetrahedral ones, Beus (1960) and Evans and Mrose (1968) proposed Al-Li substitution in the octahedron. Different distributions of cations such as Fe^{2+} or Fe^{3+} in tetrahedral or channel sites have been proposed to explain the electronic absorption, infrared, or Mössbauer spectra (Wood and Nassau, 1968; Goldman et al., 1978; Price et al., 1976). A subject of controversy is also the location of alkali ions and water molecules in the open channels of the structure, where two positions ($2a$ and $2b$) are available. The general interpretation of the residual electronic density in these sites has been that H_2O occupies the 0, 0, ¼ ($2a$) position, as well as the larger alkali ions (Cs^+, Rb^+, and K^+); the smaller Na^+ ions would lie at 0, 0, 0 ($2b$), i.e., at the center of Si rings (Hawthorne and Černý, 1977). A similar interpretation has been assumed also to explain the difference-Fourier maxima found in low cordierite, with similar structure

---

* To whom correspondence should be addressed.

(Cohen et al. 1977; Wallace and Wenk, 1980; Armbruster, 1985, 1986). The undoubtedly complex picture of the behavior of major and minor constituents in the beryl structure is not fully substantiated by completely adequate structural information. Whereas several refinements on anhydrous or hydrous synthetic beryls have been done (Gibbs et al., 1968; Morosin, 1972; Hazen et al., 1986, for the high-pressure structure), quite surprisingly very few accurate single-crystal structural determinations have been published on natural beryls: only two Cs-rich beryls have been described (Bakakin et al., 1970; Hawthorne and Černý, 1977). Another refinement on a Cs-rich beryl was announced by Evans and Mrose (1968); the structure of a natural beryl was reported by Solovyeva and Bakakin (1966). Recently a hydrous alkali-rich beryl was studied at different temperatures by Brown and Mills (1986). With the idea that a thorough study of the structures of natural beryls could offer the basis for the understanding of crystal-chemical behavior of this mineral family, we started with chemical and structural determinations on some samples from different sources and with dissimilar chemical contents.

SAMPLE DESCRIPTIONS

The 30 beryl samples studied in this work are described in Table 1: 28 are natural beryls from different deposits and geneses; 2 are synthetic beryls grown in our laboratory by flux method in $Li_2Mo_2O_7$ (Flamini et al., 1983). Several samples come from sources described in the literature. For some of them, partial or complete chemical analyses were available. Sample 6 was obtained from the Smithsonian Institution (no. 117199) as the "unusual" beryl described by Schaller et al. (1962), but our chemical results don't agree with the published analysis. Samples 7 and 8 are fragments taken from the core and the rim of the zoned red beryl from Utah. This beryl, found in a rhyolite, as described by several authors (Hillebrand, 1905; Shigley and Foord, 1985), is peculiar in that it is the unique natural beryl so far discovered with no water, as inferred by the infrared spectra (Nassau and Wood, 1968). Sixty-five complete and reliable analyses, reported in the papers by Schaller et al. (1962), Ganguli (1968), Bakakin et al. (1970), Hall and Walsh (1971), De Almeida Sampaio Filho et al. (1973), Hawthorne and Černý (1977), Barabanov (1980), Brown and Mills (1986), Ghera and Lucchesi (1987), and Lucchesi and Mairani (1987), after recalculation according to our partition criteria, were used for statistical comparisons and correlations and are plotted together with our data.

EXPERIMENTAL DETAILS

Analytical procedures

Chemical analyses were performed with the electron-microprobe analyzer JEOL JXA-50A equipped with two crystal spectrometers (WDS) and with the LINK SYSTEMS 860 energy-dispersive spectrometer (EDS). Operating conditions were 15-kV accelerating voltage and 2-nA and 20-nA specimen current for EDS and WDS, respectively. The analyses were carried out mainly by EDS, with Na and Mg contents also determined by WDS. Spot size was about 4 μm to minimize the volatilization of light elements. Synthetic diopside (Mg, Si, and Ca), corundum (Al), olivine (Fe), rutile (Ti), jadeite (Na), orthoclase (K), pollucite (Cs), and pure elements (Mn, Cr, and V) were used as standards. The data correction was obtained using the ZAF-4 FLS programs supplied by LINK SYSTEMS. At least 20 analyses for each sample were run to obtain a representative mean value over the whole crystal. Be, Li, and Rb were analyzed by a Perkin Elmer 5000 spectrometer equipped with graphite crucible. The procedures suggested by Bernas (1968) and De Almeida Sampaio Filho et al. (1973) were employed to dissolve the beryls and to determine the analytical conditions. To avoid matrix interferences, standards of similar composition were used. The water content was determined by weight loss on ignition (L.O.I.). The weight-loss determination was carried out by thermal gravimetric analyses (TGA), on about 5 mg of material for each specimen, with a TGS-2 Perkin Elmer thermogravimetric system. The temperature range was 25–900 °C; the thermal gradient was 10 °C·min⁻¹ in static air. The results of the chemical analysis are given in Table 2, together with the structural formulae recalculated on the basis of 18 oxygens. The cation partitioning among different structural sites was made taking into account our single-crystal evidence. The total Fe content from the microprobe results was subdivided into Fe^{2+} and Fe^{3+} on the basis of charge balance.

Lattice parameters and refractive indices

The unit-cell parameters of the samples not subjected to single-crystal analysis were obtained by the powder method. An automatic Seifert MZIV diffractometer equipped with Ni-filtered CuKα radiation was employed. Pure Si powder was used as internal standard. The effects of preferred orientation were eliminated by reducing the dimensions of the grains to 10 μm and rotating the samples. At least 25 univocally indexed diffraction lines were used to refine the cell dimensions by the least-squares method (Appleman and Evans, 1963). The results are given in Table 3. Some samples showed weak diffraction lines that could not be indexed on the basis of the beryl hexagonal lattice. This was ascribed to some inclusions in the crystals and not to an actual lowering of the crystal symmetry. This was confirmed also by TEM studies on one "anomalous" specimen (M. Mellini, pers. comm.) showing only a mosaic spreading of hexagonal domains.

The ω and ε refractive indices were measured with a Kruss refractometer using Na light, with an accuracy of ±0.003. The resulting values are listed in Table 3.

Single-crystal X-ray measurements and structure refinements

Among the 30 specimens from different sources at our disposal, we chose 15 for single-crystal X-ray analysis: two synthetic beryls, some beryls with high contents of divalent cations (Fe and Mg), two lithian-sodic beryls, some Li-Cs–rich beryls, and the anhydrous red beryl from Utah.

Single crystals for the X-ray work were mounted on the goniometric head of a Philips PW1100 automatic four-circle diffractometer equipped with graphite-monochromatized MoKα radiation (λ = 0.71069 Å). Since beryl crystals are often zoned, particular care was taken in the choice of the fragments. To obtain the best correlation between structural and chemical data, when possible the fragments were taken from the small chips used for the microprobe analysis. In other cases, the same crystals used in the X-ray measurements were analyzed after data collection.

TABLE 1. Description, localities, assemblages, and selected references for beryl specimens

No.	Description	Occurrence	Geologic environment and reference	Mineral association
1	Dark blue	Calcaferro mine, Pietrasanta, Tuscany, Italy	Weakly metamorphic greenschist facies with interlayered bed or lenses of quartzites and carbonate rocks "Unità di Fornovolasco-Panie" (this work)	Pyrite, barite
2	Light blue	Calcaferro mine, Pietrasanta, Tuscany, Italy	Same as no. 1	Dolomite, barite, quartz, magnetite, and hematite
3	Dark blue, zoned	South side of Mount Cervandone, Val d'Ossola, Piedmont, Italy	Feldspatic vein crossing the "Monte Leone gneiss" (Hänni, 1980)	Feldspar
4	Dark green, zoned	Mingora, Swat Valley, Pakistan	Quartz-calcite-talc pockets in dolomitic talc schist intruded by serpentinized ultramafic dikes (Gubelin, 1982)	Quartz, schorl, talc, ankerite, calcite
5	Light green	Pizzo Marcio, Val Vigezzo, Piedmont, Italy	Desilicated albitic pegmatite and serpentinite (Hänni, 1980)	Albite, bertrandite, chlorite, scheelite, pyroclore
6	Blue	Mohave County, Arizona, U.S.A. No. 117199, Smithsonian Institution	Granitic pegmatite (Schaller et al., 1962)	Schorl, quartz, feldspar
7–8	Zoned pink to red from rim to core	Violet Claims, Wah Wah Mountains, Beaver County, Utah, U.S.A.	Kaolinized rhyolite (Shigley and Foord, 1985)	Feldspar, quartz, bixbyite
9	Green	Carnaiba, Bahia, Brazil	Biotite schist (Sauer, 1982)	Quartz, phlogopite, apatite, biotite, molibdenite
10	Dark green	Muzo, Colombia	Dolomite-calcite veins imbedded in black pyritiferous argillites intercalated with limestone (Keller, 1981)	Calcite, dolomite, ankerite, parisite, aragonite, pyrite, quartz, apatite
11	Pale green	Jos, Nigeria	Pegmatite (Lind et al., 1984)	Feldspar, quartz
12	Blue	Karoi, Miami district, Zimbabwe	Pegmatite (pers. comm. of dealer)	Feldspar, quartz, lepidolite
13	Light blue	Mursinka, Ural Mountains, USSR	Pegmatite (Sinkankas, 1981)	Feldspar, quartz, schorl
14	Light blue	Nuristan, Afghanistan	Pegmatite (Bariand and Poullin, 1978)	Quartz, schorl, feldspar
15	Very pale blue	Cava Grignaschi, Trontano, Val d'Ossola, Piedmont, Italy	Pegmatite (this work)	Quartz, feldspar, bavenite, tanteuxenite
16	Yellow	Fort Victoria field, Zimbabwe	Granitic albitized pegmatite (Tynsdale-Biscoe, 1952)	Muscovite, lepidolite, cassiterite, tourmaline
17	Very pale blue	S. Piero in Campo, Isola d'Elba, Tuscany, Italy	Pegmatite (this work)	Feldspar, quartz
18	Pale pink	Mount Bity region, Madagascar	Pegmatite (Sinkankas, 1981)	Feldspar, quartz, elbaite
19	Light blue (core of no. 20)	Minas Gerais, Salinas mine, Brazil	Pegmatite (Proctor, 1984)	Feldspar, quartz, elbaite, albite, lepidolite
20	Pale pink (rim of no. 19)	Minas Gerais, Salinas mine, Brazil	Pegmatite (Proctor, 1984)	Same as no. 19
21	Colorless	Minas Gerais, Salinas mine, Brazil	Pegmatite (Proctor, 1984)	Same as no. 19
22	Pink	Nuristan, Mawi mine, Afghanistan	Pegmatite (Bariand and Poullin, 1978)	Feldspar, quartz, elbaite, spodumene
23	Green	Habachtal, Untersulzbachtal, Salzburg, Austria	Biotite, talc, and actinolite schists between serpentinites and metapelites or metavolcanic rocks near the central gneiss (Franz et al., 1986)	Biotite, actinolite, oellacherite, quartz, schorl, bertrandite, pyrite, dolomite, galena, phenakite, chrysoberyl
24	Green	Morrua, Zambesia	Biotite schist (Gubelin, 1982)	Biotite, quartz
25	Pale pink rosterite	S. Piero in Campo, Isola d'Elba, Tuscany, Italy	Pegmatite (this work)	Lepidolite, pollucite, petalite, quartz
26	Light green	Ural Mountains, USSR	Biotite schists (Vlasov and Kutukova, 1960)	Biotite, actinolite
27	Pink	Mujane mine, Zambesia	Pegmatite (Hutchinson and Claus, 1956)	Feldspar, quartz, muscovite
28	Pale pink	Pala, California, U.S.A.	Pegmatite (Jahns and Wright, 1951)	Feldspar, quartz, elbaite, lepidolite
S1	Colorless		Flux-fusion synthesis	
S2	Dark green		Flux-fusion synthesis	

The cell parameters were determined by the least-squares method applied to the θ values of about 30 reflections measured with the routine LAT of the diffractometer. The lattice constants and the cell volumes are reported in Table 3. For each crystal about 1300–1800 reflections from equivalent sectors of reciprocal space were measured in the 2–35° θ range by the ω-2θ scan technique. The intensity data were corrected for Lorentz and polarization factors. An absorption correction was applied according to the semiempirical method of North et al. (1968); the values of the corrected intensities were merged to obtain a "unique" set of independent data. R_{eq} were in the range 0.01–

0.03, again showing that the symmetry of the beryl samples is actually hexagonal. For each sample a number of reflections ranging between 400 and 550 with $I > 3\sigma(I)$ was employed in the least-squares refinement. The computations were carried out with the full-matrix program in the SHELX-76 crystallographic package (Sheldrick, 1976) starting from the atomic coordinates of synthetic beryl, space group $P6/mcc$ (as determined by Gibbs et al., 1968). Individual anisotropic thermal parameters were refined for each atom. After several least-squares cycles, difference-Fourier maps were calculated. All natural samples showed intrachannel residual maxima of electronic density in positions
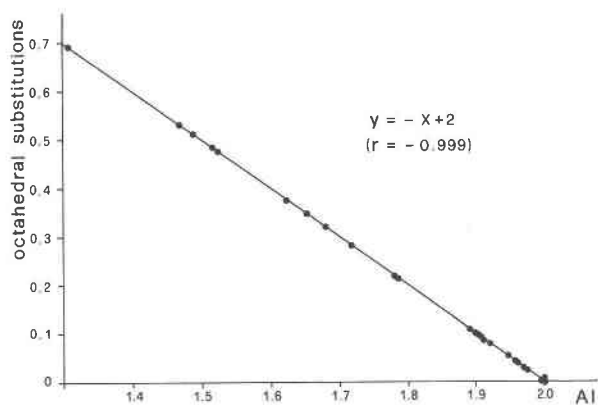
Fig. 1. Linear correlation between octahedral Al content and "octahedral substitutions," i.e., the sum of Fe^{2+} and Mg (plus minor Fe^{3+}, Cr^{3+}, V^{3+}, Mn^{2+}, Ti^{4+}). Atoms per 18 O.

Fig. 2. Linear correlation between Be and Li. Atoms per 18 O.

where alkali ions and/or water molecules are expected: a distribution of the scattering material over these sites was made on the basis of the microprobe analysis. The criteria adopted will be described later. For the atoms in tetrahedral and octahedral sites, mixed scattering curves were employed on the basis of the chemical analysis, with the constraint that the sites be totally occupied. The scattering curves of neutral atoms were taken from the *International Tables for X-ray Crystallography* (1974). The refinement converged to R values in the range 0.020–0.054 (mean value, 0.03). Bond lengths and polyhedral parameters are listed in Table 4. Complete listing of fractional atomic coordinates, thermal factors, and observed and calculated structure factors are given in Tables 5, 6, and 7, respectively.[1]

CHEMISTRY OF BERYL

The SiO_2 content is rather constant, varying in the range 63–66 wt%. An excess of Si atoms is often observable in the unit formulae; this excess could be ascribed to high silica activity in the crystallization environment and can be assigned to the Be tetrahedron.

Al_2O_3 shows the widest variation, ranging from 11.72 to 18.90 wt%. The deficiency of octahedral Al is correlated to Fe^{2+} and Mg (plus Fe^{3+}, Cr^{3+}, V^{3+}, Mn^{2+}, Ti^{4+}) content (Fig. 1), confirming the mutual substitution of these ions in the octahedral sites ("octahedral" beryls).

The Be content shows an opposite trend with respect to Al. It is close to the stoichiometric value in the "octahedral" beryls, where its tetrahedral site is completed by small quantities of Si (max. 0.115 atoms) or Al (max. 0.077 atoms). It becomes lower in the samples where Li content is higher. Figure 2 shows the negative correlation between Be and Li, indicating that Be is partially replaced by Li in the tetrahedral sites ("tetrahedral" beryls).

Alkali ions (R_i^+) enter the beryl structure to satisfy charge deficiencies, and their content is correlated with the amount of substitutions in the octahedral and tetra-
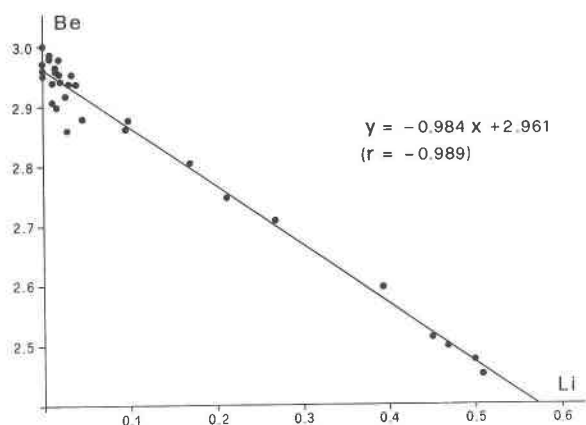
hedral sites. Taking into account the substitutions with ions carrying charge unlike that of the main cations, the following equation can be written:

$$R_f = [Al(T'')] + [Fe^{2+}] + [Mg] + [Mn]$$
$$- [Ti] - 2[Si(T')] - [Al(T')] + [Li], \quad (1)$$

where T' and T'' are the tetrahedral sites of Be and Si, respectively (brackets without a site symbol refer to octahedral sites).

Figure 3 shows the correlation between Cs, Rb, K, and Na and the sum of cations of the right side of Equation 1. Of these alkali elements, Na is always present, whereas Cs is present especially in the Li-rich beryl, as observed by Bakakin and Belov (1962). Rb and K are near to the detection limits, with the exception of the red beryl from Utah (samples 7 and 8), which is K-rich, probably because of its genesis (Aurisicchio et al., 1986). Minor amounts of Cr_2O_3, MnO, TiO_2, and V_2O_5 were sometimes observed as traces. They are expected to play an important role in beryl coloring.

REFINEMENT RESULTS

Synthetic beryls

The two synthetic samples give very similar results. The geometry for Si, Al, and Be polyhedra is in perfect agreement with the results reported by Gibbs et al. (1968) and Morosin (1972) for the analogous compounds.

In particular the Si tetrahedron shares two vertices through O(1) with neighboring tetrahedra to form a hexagonal ring, and two vertices [O(2)] with two different Be tetrahedra and Al octahedra. As observed by Gibbs et al., despite the differences in bond lengths [Si–O(1) and Si–O(2) average 1.594 and 1.622 Å, respectively], the tetrahedral angles are close to the ideal value: the bond-angle variance, σ^2 (Robinson et al., 1971), is 1.6 deg². The bond-valence sums for O(1) and O(2), computed with the method of Brown and Wu (1976), are 2.07 and 1.96, respectively.

In contrast, the 4-fold coordination polyhedron around

TABLE 2. Chemical analyses of the beryls described in Table 1

	3	1	2	4	6	5	23	24	7	9	13	8	10	11
SiO_2	64.42	64.63	64.93	64.77	64.24	65.16	63.60	64.69	66.15	65.18	65.59	66.45	65.34	65.66
Al_2O_3	11.72	14.10	13.63	13.63	14.95	14.25	14.54	16.05	15.99	16.57	18.25	18.02	16.51	17.90
FeO	4.62	3.83	2.22	1.22	2.97	0.76	0.38	0.81	2.25	0.50	1.16	1.06	0.31	1.26
MnO	—	—	—	—	—	—	—	—	0.64	—	—	0.17	—	—
MgO	2.31	1.27	2.44	2.60	0.82	3.08	2.27	1.86	0.17	1.15	—	—	0.87	—
Cr_2O_3	—	—	—	0.98	—	—	0.35	—	—	0.26	—	—	0.37	—
V_2O_5	—	—	—	—	—	—	—	—	—	—	—	—	0.64	—
TiO_2	—	—	—	—	—	—	—	—	0.55	—	—	—	—	—
Na_2O	2.21	2.35	2.46	1.90	1.73	2.25	1.72	1.35	0.30	1.15	0.26	0.35	0.49	—
K_2O	—	—	—	—	—	—	—	—	0.22	—	—	—	—	—
Cs_2O	0.31	—	—	—	0.99	—	—	—	0.33	—	—	0.38	—	—
Rb_2O	—	—	—	—	—	—	—	—	0.10	—	—	0.06	—	—
Li_2O	0.07	0.07	0.05	0.03	0.26	0.12	0.04	0.04	0.03	0.10	—	0.04	—	0.02
BeO	12.55	13.02	13.18	12.96	12.77	12.94	13.01	13.00	13.40	13.27	13.46	13.66	13.37	13.61
L.O.I.	1.70	n.d.	n.d.	2.20	1.50	2.00	2.60	2.00	0.00	2.30	0.70	0.00	2.40	1.10
Total	99.91	99.27	98.91	100.29	100.23	100.56	98.51	99.80	100.13	100.48	99.42	100.19	100.30	99.55
							T" site							
Si	6.000	6.000	6.000	6.000	6.000	6.000	6.000	6.000	6.000	6.000	5.993	6.000	6.000	5.991
Al	—	—	—	—	—	—	—	—	—	—	0.004	—	—	0.009
							Octahedral site							
Al	1.307	1.525	1.489	1.470	1.652	1.516	1.623	1.680	1.718	1.784	1.911	1.907	1.782	1.904
Fe^{3+}	0.074	—	0.011	—	0.040	0.012	—	—	0.030	—	0.002	0.003	—	0.096
Fe^{2+}	0.292	0.299	0.162	0.095	0.193	0.047	0.030	0.063	0.142	0.038	0.085	0.077	0.024	—
Mn	—	—	—	—	—	—	—	—	0.049	—	—	0.013	—	—
Mg	0.327	0.177	0.338	0.362	0.115	0.425	0.320	0.257	0.023	0.159	—	—	0.119	—
Cr	—	—	—	0.072	—	—	0.026	—	—	0.019	—	—	0.027	—
V	—	—	—	—	—	—	—	—	—	—	—	—	0.047	—
Ti	—	—	—	—	—	—	—	—	0.038	—	—	—	—	—
							T' site							
Be	2.859	2.916	2.942	2.907	2.876	2.879	2.960	2.899	2.940	2.937	2.953	2.965	2.960	2.982
Li	0.027	0.026	0.019	0.011	0.098	0.045	0.015	0.015	0.011	0.037	—	0.014	—	0.007
Si	0.111	0.029	0.036	0.050	0.025	0.037	0.025	0.008	0.045	0.008	—	0.007	0.025	—
Al	0.003	0.025	0.004	0.030	—	0.040	—	0.077	0.004	0.016	0.047	0.012	0.012	0.012
							2a site							
R_I	0.418	0.425	0.443	0.344	0.355	0.404	0.316	0.243	0.095	0.206	0.046	0.078	0.088	—
Na	0.406	0.425	0.443	0.344	0.315	0.404	0.316	0.243	0.053	0.206	0.046	0.061	0.088	—
K	—	—	—	—	—	—	—	—	0.026	—	—	—	—	—
Cs	0.012	—	—	—	0.040	—	—	—	0.013	—	—	0.015	—	—
Rb	—	—	—	—	—	—	—	—	0.003	—	—	0.002	—	—

Note: Atomic proportions are computed on the basis of 18 oxygens. The natural samples are listed in order of increasing c/a ratio. L.O.I. = loss on ignition; n.d. = not determined; dash = below detection; Fe^{3+} by charge balance.
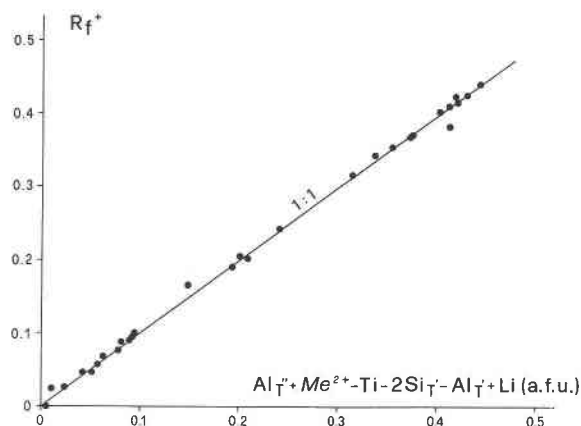

Fig. 3. Correlation between alkali content of the channels ($R_I^+ = Cs^+ + Rb^+ + K^+ + Na^+$) and the sum of divalent cations, Li^+, and the other ions listed in the right side of Equation 1. Atoms per 18 O.

Be is strongly distorted; the four equivalent Be–O(2) bond lengths are 1.656 Å, with a tetrahedral bond-angle variance of 331 deg^2.

Also the 6-fold polyhedron around Al is distorted, with six equivalent Al–O(2) distances of 1.906 Å. Each coordination polyhedron around Al shares three edges with three different Be tetrahedra. These edges are shorter than the other edges of the polyhedron (2.359 Å versus 2.848 and 2.712 Å). The resulting geometry for the Al polyhedron is that of an octahedron flattened along [001]. The quantification of the distortion in the octahedron can be achieved through the bond-angle variance, which is 74.5 deg^2.

Natural beryls

First of all let us consider the results from the refinement of the Utah red beryl. As the crystals are zoned, two fragments—one from the core and one from the rim of the crystal—were chosen for the X-ray single-crystal study (samples 7 and 8). After several cycles of least-

TABLE 2—*Continued*

12	14	26	15	16	17	25	28	18	21	19	27	22	20	S1	S2
65.73	65.92	65.14	65.75	66.17	66.72	63.99	65.67	65.22	64.16	63.20	63.54	63.29	63.10	66.32	66.48
17.74	17.85	17.72	17.75	18.52	18.54	18.19	18.82	18.35	18.06	17.95	17.92	17.76	17.93	18.76	18.90
1.20	0.82	0.24	0.57	0.32	0.50	—	—	—	—	—	—	—	—	0.53	—
—	—	—	—	—	—	0.37	—	—	—	—	—	—	—	—	—
—	0.32	0.44	0.42	—	—	—	—	—	—	—	—	—	—	—	0.74
—	—	—	—	—	—	—	—	—	—	—	—	—	—	—	—
—	—	—	—	—	—	—	—	—	—	—	—	—	—	—	—
—	—	—	—	—	—	—	—	—	—	—	—	—	—	—	—
0.38	0.57	0.51	0.51	0.15	0.26	0.55	0.77	1.01	1.57	1.30	1.44	1.23	1.41	0.27	0.14
—	—	—	—	—	—	—	—	—	—	—	—	—	—	—	—
—	—	—	—	—	0.30	2.27	0.76	0.57	2.10	3.24	3.97	3.79	3.68	—	—
—	—	—	—	—	—	—	—	—	0.02	0.05	0.06	0.05	0.04	—	—
0.08	0.05	0.05	0.09	0.02	0.26	0.56	0.46	0.72	1.19	1.03	1.33	1.30	1.22	—	—
13.34	13.52	13.46	13.46	13.71	13.18	12.19	12.79	12.20	11.12	11.38	10.74	10.79	10.90	13.88	13.78
1.10	0.90	2.30	1.00	1.10	0.80	0.90	0.90	0.30	1.30	1.20	1.00	1.10	1.40	0.00	0.00
99.57	99.95	99.86	99.55	99.99	100.56	99.02	100.10	98.37	99.52	99.35	100.00	99.31	99.68	99.76	100.04
						T'' site									
6.000	6.000	6.000	6.000	6.000	6.000	6.000	5.996	6.000	6.000	6.000	6.000	6.000	6.000	5.971	5.969
—	—	—	—	—	—	—	0.004	—	—	—	—	—	—	0.029	0.031
						Octahedral site									
1.908	1.894	1.921	1.900	1.976	1.962	1.971	2.000	2.000	2.000	2.000	2.000	1.998	2.000	1.960	1.947
—	0.004	—	0.023	—	—	—	—	—	—	—	—	—	—	0.017	—
0.092	0.059	0.018	0.020	0.024	0.038	—	—	—	—	—	—	—	—	0.023	—
—	—	—	—	—	—	0.029	—	—	—	—	—	—	—	—	—
—	0.043	0.060	0.057	—	—	—	—	—	—	—	—	—	—	—	0.053
—	—	—	—	—	—	—	—	—	—	—	—	—	—	—	—
—	—	—	—	—	—	—	—	—	—	—	—	—	—	—	—
						T' site									
2.937	2.956	2.978	2.952	2.986	2.861	2.746	2.804	2.708	2.512	2.596	2.450	2.474	2.497	3.001	2.971
0.029	0.018	0.018	0.033	0.007	0.094	0.211	0.169	0.268	0.450	0.393	0.508	0.499	0.468	—	—
0.025	0.002	0.001	0.005	0.002	0.031	0.003	—	0.029	0.037	0.004	0.036	0.043	0.020	—	—
0.008	0.021	0.003	0.011	0.004	0.013	0.040	0.020	—	0.002	0.009	0.006	—	0.016	0.001	0.021
						$2a$ site									
0.067	0.101	0.091	0.090	0.026	0.058	0.191	0.166	0.203	0.371	0.372	0.428	0.384	0.412	0.047	0.024
0.067	0.101	0.091	0.090	0.026	0.046	0.100	0.136	0.181	0.286	0.239	0.265	0.228	0.261	0.047	0.024
—	—	—	—	—	0.012	0.091	0.030	0.022	0.084	0.131	0.161	0.154	0.150	—	—
—	—	—	—	—	—	—	—	—	0.001	0.002	0.002	0.002	0.001	—	—

squares refinement, a difference-Fourier synthesis for both samples showed two peaks of residual electronic density, at the position of the octahedral site and in the $2a$ position, i.e., at 0, 0, ¼ in the channel between the Si rings. No maxima were detected in the $2b$ position, i.e., at 0, 0, 0 at the ring center. The refinement was therefore continued by including the contribution of K and Na at the site $2a$ and of Fe (and Mg and Mn) in the octahedral site, in the amounts determined by the microprobe analysis. The final agreement between observed and calculated structure factors was very satisfactory ($R = 0.020$ for both crystals). Since the Utah beryl is the unique natural beryl with no water content, a tentative hypothesis was that the alkali ions (the so called R_i^+ ions = Cs^+, Rb^+, K^+, Na^+), when present in beryls, occupy exclusively the $2a$ site, whereas the water molecules always present in the other natural beryls preferentially lie in $2b$ sites. This conclusion contrasts with that reported by Hawthorne and Černý (1977) and later used by Brown and Mills (1986) to interpret the residual electron density in the Harding ber-

yl. The crystal-chemical validity of this hypothesis, already argued by Bakakin and Belov (1962), is supported also by the geometry features of the $2b$ sites, which have an atomic environment similar to the centers of the hexagonal oxygen rings in layer silicates or in amphiboles: water molecules would complete the closest packing of oxygen layers and could act as "support" for small cations like Na or Ca possibly present in $2a$ sites. The distance between the center of the ring and the oxygen atoms (about 2.55 Å) corresponds to a short hydrogen-bond, and this fact, together with the presence of alkali ions "plugging" the channels, could explain the unusually high temperature necessary to release this "zeolitic" water in beryl (e.g., Aines and Rossman, 1984; Brown and Mills, 1986). Both hypotheses on the H_2O location are probably valid, and actually water molecules may well occupy $2a$ as well as $2b$ positions in the channels. This could explain the presence in the infrared spectra of two H_2O types (Wood and Nassau, 1967; Polupanova et al., 1985) that have been explained as being due to two different orien-

TABLE 3. Lattice parameters (Å), c/a ratio, cell volumes (Å³), and refractive indices of the beryls listed in Table 1

No.	a	c	c/a	V	ω	ε
3	9.2736(11)	9.1910(25)	0.9911	684.5	1.603	1.595
1	9.2666(5)	9.1874(4)	0.9915	683.2	n.d.	n.d.
2	9.2676(6)	9.1945(3)	0.9921	683.9	n.d.	n.d.
4	9.263(1)	9.199(1)	0.9931	683.6	1.599	1.590
6	9.2531(7)	9.1918(5)	0.9934	681.6	n.d.	n.d.
5	9.257(1)	9.201(1)	0.9940	682.8	1.591	1.585
23	9.249(1)	9.200(1)	0.9947	681.6	1.591	1.584
24	9.2367(1)	9.1903(2)	0.9950	679.0	1.589	1.582
7	9.2364(8)	9.1933(4)	0.9953	679.2	1.580	1.575
9	9.226(1)	9.192(1)	0.9963	677.6	1.587	1.580
13	9.2179(14)	9.1863(9)	0.9966	676.0	1.576	1.570
8	9.2242(3)	9.1934(2)	0.9967	677.4	1.571	1.568
10	9.218(1)	9.189(1)	0.9969	676.2	1.580	1.576
11	9.219(1)	9.192(1)	0.9971	676.6	1.578	1.570
12	9.2202(10)	9.1960(6)	0.9974	677.0	1.588	1.581
14	9.220(1)	9.197(1)	0.9975	677.1	1.585	1.580
26	9.2176(5)	9.1968(3)	0.9977	676.7	1.582	1.576
15	9.217(1)	9.196(1)	0.9977	676.4	1.586	1.580
16	9.2097(12)	9.1943(7)	0.9983	675.4	1.580	1.577
17	9.215(1)	9.200(1)	0.9984	676.6	1.589	1.585
25	9.216(1)	9.207(1)	0.9990	677.2	1.590	1.583
28	9.213(1)	9.212(1)	0.9999	677.1	1.586	1.580
18	9.215(1)	9.218(3)	1.0003	677.9	1.589	1.580
21	9.218(1)	9.230(1)	1.0013	679.2	1.594	1.589
19	9.2155(8)	9.2291(5)	1.0015	678.8	1.590	1.583
27	9.217(1)	9.233(1)	1.0017	679.3	1.598	1.590
22	9.2148(3)	9.2318(4)	1.0018	678.9	1.597	1.589
20	9.2097(4)	9.2337(4)	1.0026	678.3	1.595	1.587
S1	9.2077(6)	9.1953(5)	0.9987	675.1	n.d.	n.d.
S2	9.2051(5)	9.1953(4)	0.9989	674.8	n.d.	n.d.

Note: Estimated standard deviations in parentheses refer to the last digit; n.d. = not determined. The cell constants reported with four decimal places were determined by the single-crystal method.

tations of the H-H vector. It is also possible that water occupies the $2a$ sites as the complex H_3O^+ ion, balancing the positive charge deficiency due to either trivalent-divalent substitution in the octahedron or Li$^+$ entry in the Be tetrahedron. However, the hypothesis that H_2O molecules occupy preferentially the $2b$ sites was satisfactorily

used as a criterion to distribute the alkali cations (Na, K, Rb, and Cs) and the water molecules in the channel sites during the refinement of the other natural beryls. All these crystals present residual electron-density maxima in the $2a$ and $2b$ positions, which can be accounted for with the amounts of alkali ions from microprobe analysis (in $2a$) and with 0.6–0.7 H_2O molecules per formula unit (in $2b$).

CRYSTAL CHEMISTRY

The results of the single-crystal X-ray study on our synthetic and natural beryls, as well as those taken from the accurate determinations reported in the literature, were subjected to statistical analysis. Some of the most significant correlation coefficients among chemical and structural parameters are listed in Table 8.

It is confirmed that two kinds of cationic substitutions take place in natural beryls: those in the distorted octahedron and those in the BeO$_4$ tetrahedron.

Substitutions in distorted octahedron

The Al^{3+} in the distorted octahedral site can be substituted for by ions of comparable size; among these ions the most important ones are Mg^{2+} and Fe^{2+}, with minor Mn^{2+}, Cr^{3+}, Fe^{3+}, Ti^{4+}, and other less abundant atomic species. The substitution for Al by Mg and/or Fe has two main effects on the structure: the volume of the polyhedron must increase to receive ions with greater radii, therefore an elongation of Me–O distances would be expected as well as an increase in the distortion of the polyhedron, since the length of the edges shared with BeO$_4$ adjacent groups is constrained by the dimensions of the Be tetrahedron. Furthermore, the Al $\rightleftharpoons$ Me^{2+} substitution would have the effect of reducing the distortion in the BeO$_4$ group. These effects are actually observed; from the statistical analysis of our results, there are positive correlations among the content of divalent ions, the cation–oxygen distance, the volume of the site, and the octahe-

TABLE 4. Bond distances (Å), site volumes, bond-angle variance σ^2 (deg²), agreement factors, and number of reflections used in the least-squares refinements

	S1	S2	1	2	3	6	7	8	12	16
					T″ site					
Si–O(1)	1.594(1)	1.593(1)	1.605(2)	1.606(1)	1.603(2)	1.601(2)	1.598(1)	1.596(1)	1.595(1)	1.595(2)
–O(1)	1.594(1)	1.593(1)	1.604(2)	1.605(1)	1.602(2)	1.603(2)	1.594(1)	1.595(1)	1.601(1)	1.595(1)
–O(2) × 2	1.622(1)	1.621(1)	1.617(1)	1.614(1)	1.616(2)	1.615(1)	1.621(1)	1.621(1)	1.617(1)	1.621(1)
Mean	1.608	1.607	1.611	1.610	1.609	1.608	1.609	1.608	1.608	1.608
V (Å³)	2.133	2.129	2.142	2.135	2.136	2.132	2.134	2.133	2.129	2.132
σ²	1.58	1.62	4.46	5.44	3.26	3.61	1.44	1.64	2.58	1.58
					T′ site					
Be–O(2) × 4	1.656(1)	1.655(1)	1.654(1)	1.653(1)	1.650(2)	1.655(1)	1.655(1)	1.656(1)	1.659(1)	1.655(1)
V (Å³)	2.031	2.035	2.065	2.073	2.060	2.070	2.050	2.042	2.053	2.031
σ²	333	328	289	276	275	290	313	323	322	332
					Octahedral site					
Al–O(2) × 6	1.905(1)	1.906(1)	1.938(1)	1.943(1)	1.947(2)	1.933(1)	1.920(1)	1.913(1)	1.913(1)	1.906(1)
V (Å³)	8.929	8.943	9.322	9.427	9.478	9.297	9.127	9.036	9.043	8.945
σ²	74.6	74.4	84.7	85.0	87.2	81.5	78.2	76.1	73.9	74.7
R	0.027	0.021	0.029	0.031	0.048	0.024	0.020	0.020	0.032	0.054
No. obs.	502	486	469	466	489	419	478	475	453	450

Note: Estimated standard deviations (in parentheses) refer to the last digit.

dral bond-angle variance. In Figure 4 the octahedral Me–O distance is plotted against the content of divalent cations; the correlation coefficient is 0.98. To attain the electric neutrality, the substitution of trivalent cations with divalent ones is compensated by some alkali ions in the channels. These ions lie in the $2a$ position and are weakly linked to O(1). They induce a distortion in the Si tetrahedra, as seen by the increase of bond-angle variance with total alkali content in the channels (correlation coefficient = 0.86). Since the $2a$ position has twofold multiplicity in the hexagonal cell of the beryl, there is an upper limit of one alkali ion per 6 Si atoms, i.e., an upper limit of one divalent ion in the two octahedral sites of the formula. Alkali ions do not contribute to the total valence sum on the O(2) atoms, which will be to some extent unbalanced. A partial compensation is achieved by the shortening of Si–O(2) bond length, but an extended diadochy is hampered. In the beryl from Cervandone (sample 3), which is the richest in divalent cations in our series, the valence sum of O(2) is 1.87. For this reason, we think that the $Al^{3+} \rightleftharpoons Li^+$ substitution is highly unfavored and, therefore, is highly unlikely.

Substitutions in BeO_4 tetrahedron

In the BeO_4 tetrahedron, the high correlation coefficient between the cation–oxygen distance and Li content, as well as the correlation shown in Figure 2, indicates that Li enters the framework of beryl in substitution for Be. This confirms the model of Bakakin et al. (1969), the negative correlation between Li and Be concentration observed by De Almeida Sampaio et al. (1973), and the structural results of Hawthorne and Černý (1977). As in the case of $Al \rightleftharpoons Me^{2+}$ octahedral substitution, the entry of Li^+ into the Be tetrahedron causes a bond-strength deficiency to O(2). In the Li-rich beryl from Afghanistan (sample 22), the valence sum of O(2) is 1.86. Also in this case, the electric neutrality is attained by the entry of alkali ions of suitable radii into the channels, and there-
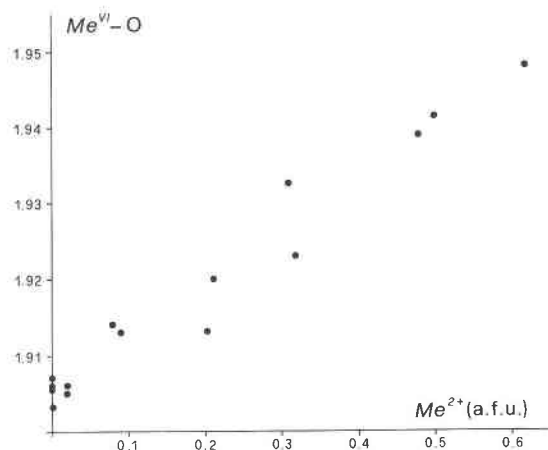
Fig. 4. Correlation between the cation–oxygen distance in the octahedron (Å) and the sum of divalent cations. Atoms per 18 O.

fore there is an upper limit in the Be $\rightleftharpoons$ Li substitution; only one-third of the tetrahedral positions can be occupied by Li^+. The substitution of Li for Be—increasing the cation–oxygen distances and the volume of the Be tetrahedron—partially releases the strain on the adjacent octahedron; the O(2)-O(2) short edge increases in length from 2.359 Å in synthetic beryl to 2.387 Å in sample 22, which has 0.51 atom of Li per formula unit. Consequently, the octahedral bond-angle variance decreases to 63.4 deg^2.

Si tetrahedron

For the Si tetrahedron, all the refined beryls have the same mean Si–O bond length (1.609 ± 0.002 Å). This fact indicates uniform Si occupation at these ring positions.

Channel sites

With regard to the channel sites, the $2a$ site is occupied by alkali ions (Na^+, Cs^+, K^+, Rb^+, and perhaps by H_3O^+ and H_2O). As pointed out by Černý (1975), the kind of alkali entering the channels, in absence of specific crystal-chemical constraints, depends on the bulk chemistry of

TABLE 4—Continued

19	20	22	24	26
		T″ site		
1.603(2)	1.603(2)	1.602(1)	1.600(1)	1.593(2)
1.609(1)	1.605(2)	1.610(1)	1.601(1)	1.605(2)
1.612(2)	1.612(1)	1.614(1)	1.616(1)	1.616(1)
1.609	1.608	1.610	1.608	1.608
2.130	2.127	2.134	2.131	2.129
7.02	6.23	7.09	3.19	2.89
		T′ site		
1.674(1)	1.675(1)	1.676(1)	1.656(1)	1.657(1)
2.113	2.118	2.117	2.061	2.045
322	322	326	302	322
		Octahedral site		
1.907(1)	1.906(1)	1.903(1)	1.923(1)	1.914(1)
9.003	8.986	8.951	9.172	9.052
64.3	63.1	63.4	79.0	74.1
0.045	0.036	0.033	0.028	0.039
463	467	478	533	450

TABLE 8. The most relevant correlation coefficients between chemical and structural parameters from single-crystal refinement

	[6]Me–O(2)	T′–O(2)	a	c	$\sigma_{T'}^2$	$\sigma_{T''}^2$	σ_{oct}^2
a	0.98						
c		0.90					
Li		0.96		0.91			
Alk						0.86	
ΣMe^{2+}	0.98		0.98		–0.95		0.81

Note: a, c = lattice parameters; ΣMe^{2+}, Li, and Alk = sum of divalent cations (Fe^{2+} + Mg + Mn), Li, and alkali metals (Na + K + Rb + Cs) in the $2a$ site, respectively; [6]Me–O(2) = octahedral cation–oxygen bond distance; T′–O(2) = cation–oxygen distance in Be tetrahedron; σ^2 = bond-angle variance in T′ (Be), T″ (Si) tetrahedra, and in the Al octahedron.
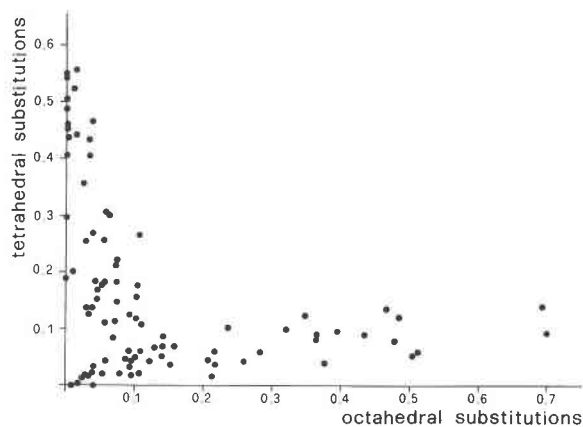
Fig. 5. The total substitutions in the Be tetrahedral site plotted against the total substitutions in the Al octahedral site. The two different series are evident.

Fig. 6. Ternary diagram based on end members $Al_2Be_3Si_6O_{18} \cdot zH_2O$ ("normal" beryl, I), $R_f^+Al_2Be_2LiSi_6O_{18} \cdot zH_2O$ ("tetrahedral" beryl, II) and $R_f^+AlMe^{2+}Be_3Si_6O_{18} \cdot zH_2O$ ("octahedral" beryl, III). Black circles: present work; open circles: analyses from literature. The dashed line represents an interpretative boundary that limits the compositional gap between "octahedral" and "tetrahedral" beryls.

the parent rock. The $2b$ site is more or less filled by H_2O molecules. Owing to the multiplicity of the $2b$ position in the hexagonal cell, the number of H_2O molecules in $2b$ can be at most equal to 1 per 6 Si atoms. When the number of H_2O molecules is higher than 1, water must occupy the $2a$ position. So the upper theoretical limit of water content in beryl is 2 minus the alkali content of $2a$ (per 6 Si). Among our samples, sample 23, which has the largest weight loss on ignition (2.60%), contains 0.79 H_2O molecules and 0.32 Na^+ ions, having the channel 56% filled. Generally, pegmatitic beryl samples have a water content of 0.3–0.6 molecules per 6 Si (Vorma et al., 1965; Černý and Simpson, 1977; present work); higher H_2O contents can be found in beryls from schists and veins. Among the 65 analyses from the literature taken into account in the present work, the most H_2O-rich beryl is from the Altai Mountains (number 24 in Bakakin et al., 1970), containing 0.9 H_2O molecules per 6 Si atoms.

Compositional gap

In Figure 5 the total substitutions in the Al octahedral site are plotted against the substitutions in the Be tetrahedral site. Two beryl series are indicated by the impossibility of finding beryls in which divalent ions substitute for trivalent ions in octahedral sites and monovalent ions *simultaneously* substitute for divalent ions in tetrahedral sites to an extent near the upper limit imposed by the maximum possible content in the channels of one alkali ion per formula unit. Figure 6, a ternary diagram having as end members $Al_2Be_3Si_6O_{18} \cdot zH_2O$ ("normal" beryl)–$R_fAlMe^{2+}Be_3Si_6O_{18} \cdot zH_2O$ ("octahedral" beryl)–$R_fAl_2Be_2LiSi_6O_{18} \cdot zH_2O$ ("tetrahedral" beryl), shows the analyses of a number of beryls. The compositional gap is evident.

Effects of substitutions on
Lattice parameters

As was shown by the statistical tests of De Almeida Sampaio Filho et al. (1973), there are direct correlations
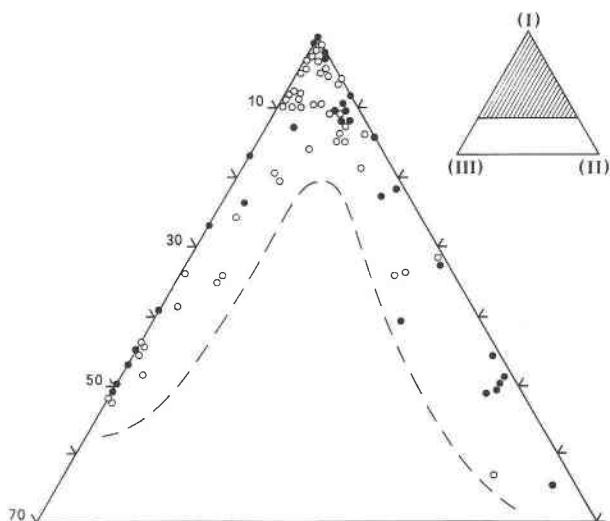
between the a unit-cell edge and the divalent-ion content and between the c unit-cell edge and the Li content in beryls. Our results confirm that observation, which can be explained by recognizing that divalent ions increase the cation–oxygen bond length in the octahedron; this octahedron, constrained by the short edges shared with Be tetrahedra, is flattened in the c direction, and therefore the increase in length influences directly the value of the a parameter. In contrast, an increase in tetrahedral cation–oxygen distance due to Li $\rightleftharpoons$ Be substitution is manifested as an increase of the length of the c axis. In Figures 7 and 8, the values of a and c unit-cell edges are plotted against the c/a ratio. The break in slope clearly distinguishes "octahedral" from "tetrahedral" beryls. From the examination of these diagrams, it appears that there are two populations of beryls: those with substitutions predominantly in the octahedral site and those with Li $\rightleftharpoons$ Be substitution in the tetrahedral site. For c/a values in the range 0.991–0.996, the Al content is sensibly lower than 2 atoms per formula unit (a.f.u.), varying from 1.305 to 1.784. In these samples, Be content is constantly near the theoretical value of 3 a.f.u. (generally more than 2.9). For c/a values in the range 0.997–0.999, Al content rises to 1.9 a.f.u. or more, and Be content is near the stoichiometric values. These beryls are "normal" beryls. For c/a values from 1.000 to 1.003, Al content becomes stoichiometric, whereas Be content decreases to 2.43 a.f.u.

The different behavior of the lattice parameters for the Al $\rightleftharpoons$ Me^{2+} and Be $\rightleftharpoons$ Li substitutions reflects the opposite distortion arising in the beryl structure with special regard to the octahedron and T' tetrahedron. These oppo-
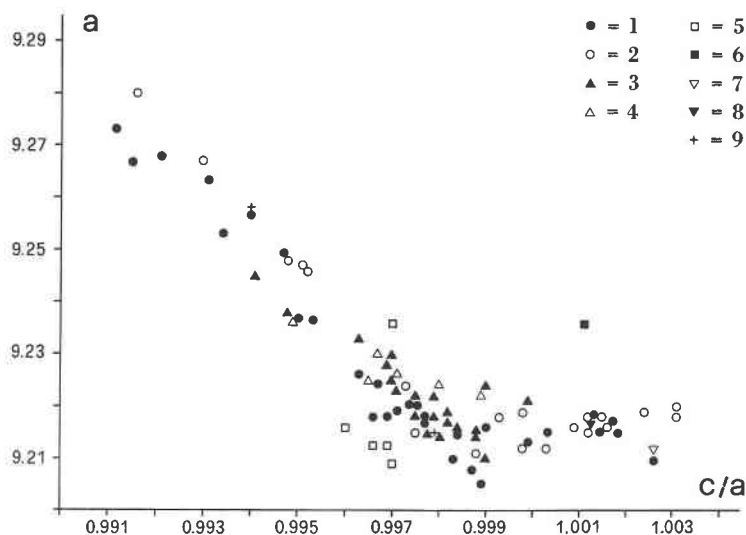
Fig. 7. The lattice parameter a (Å) vs. the c/a ratio. The different trends correspond to "octahedral" and "tetrahedral" beryls. 1 = present work; 2 = Bakakin et al. (1970); 3 = de Almeida Sampaio Filho et al. (1973); 4 = Hall and Walsh (1971); 5 = Barabanov (1980); 6 = Brown and Mills (1986); 7 = Hawthorne and Černý (1977); 8 = Vorma et al. (1965); 9 = Ghera and Lucchesi (1987) and Lucchesi and Mairani (1987).

site effects could explain why "octahedral" and "tetrahedral" substitutions form two distinct series.

CONCLUSIONS

A natural beryl can be considered as a solid solution in the ternary system between the end members (1) $Al_2Be_3Si_6O_{18} \cdot zH_2O$, (2) $R_fAlMe^{2+}Be_3Si_6O_{18} \cdot zH_2O$, and (3) $R_fAl_2Be_2LiSi_6O_{18} \cdot zH_2O$, where R_f represents Cs, Rb, K, and Na. Indeed a representative formula for a beryl could be $(R_f)_{x+y}Al_{2-x}Me_x^{2+}Be_{3-y}Li_ySi_6O_{18} \cdot zH_2O$, where the sum $x + y$ is theoretically between 0 and 1, and z is

between 0 and $2 - x - y$. These limits are imposed by the crystal structure of beryl, i.e., by the maximum possible content of alkali ions in the channels. Another limiting factor is the imbalance of O(2); "octahedral" and "tetrahedral" substitutions produce a bond-strength deficiency in bonds to O(2), and this situation lowers the allowed upper limit of $x + y$ below 1, in order to avoid a too-low valence sum on O(2). Actually the values of $x + y$ taken from our analyses and those from several accurate analyses in the literature are less than 0.5; z is normally less than 0.8 with typical values of 0.3–0.6 in
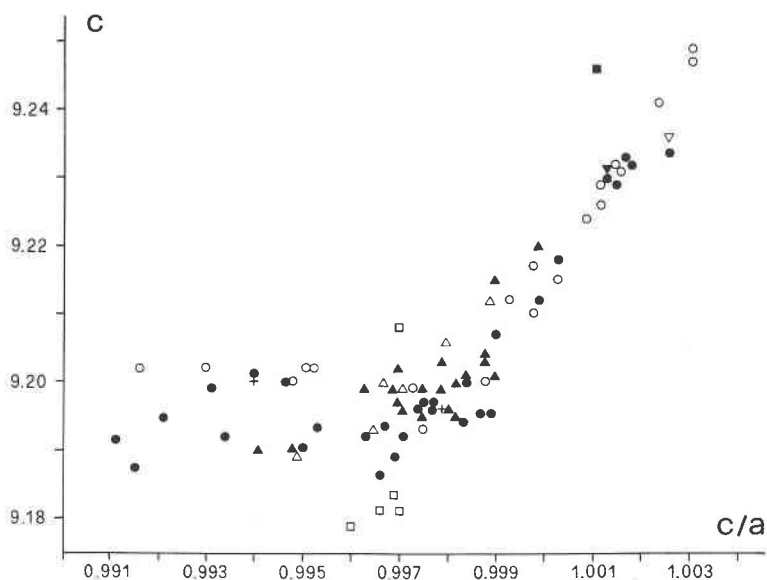

Fig. 8. The lattice parameter c (Å) plotted against the c/a ratio. The different trends correspond to "octahedral" and "tetrahedral" beryls. Symbols as in Fig. 7.

pegmatitic beryls and greater values in some beryls from veins and schists.

Indeed from a statistical study of the chemical analyses of the present work and those reported in the literature, it appears that there is a compositional gap between beryls with "octahedral" and "tetrahedral" substitutions and that known beryl compositions fall in two distinct fields (Fig. 6). The reasons why the dominant substitution in some beryls is in the octahedron whereas in others it is in the tetrahedron are not completely clear, but we suggest that there are at least two kinds of controlling factors that favor one or the other substitution. The most important factor is the chemical constraint of the environment, namely, the bulk-rock chemistry and the fluid-phase composition, as shown by the papers of Staatz et al. (1965), Černý and Turnock (1975), Černý and Simpson (1977), and Franz et al. (1986). The second factor could be ascribed to the physical-chemical conditions during the growth of the mineral, namely, the pressure and/or temperature parameters. By applying the empirical formula of Hazen and Finger (1982, p. 191), the increase in compressibility coefficient β is greater for "tetrahedral" Be $\rightleftharpoons$ Li substitution than for "octahedral" Al $\rightleftharpoons$ Mg or Al $\rightleftharpoons$ Fe substitution. This could lead to the conclusion that an increase of pressure would favor the Li entry in the framework. This idea is supported by the fact that during the growth of beryls from $Li_2Mo_2O_7$ flux under atmospheric pressure conditions (Flamini et al., 1983), crystals with some octahedral substitutions (Cr^{3+}, V^{3+}, Fe^{2+}, Co^{2+}, Mn^{2+}), but without Li, were obtained. Furthermore, this result is in agreement with the observation by Staatz et al. (1965) and Hänni (1980) that beryls from Alpine veins contain only small amounts of Cs and Li and are relatively richer in Mg, Fe, V, Cr, and Ti. Concerning the behavior of beryl with increasing temperature, the studies of Morosin (1972) on the thermal expansion of pure beryl show that the lattice parameter a regularly expands with increasing temperature, but that c undergoes a minimum around 300 °C. This minimum shifts toward lower temperature in emerald and disappears in the hydrous alkali-rich beryl studied by Brown and Mills (1986). Since the c axis is directly related to the size of Be tetrahedron and hence to its Li content, it could be argued that at relatively low temperatures, the Li substitution would be unfavored, and the entry of Mg and Fe^{2+} as substituents for Al would be preferred. Indeed, the studies by Franz et al. (1986) on the compositions of some metamorphic beryls from Austria show that the increase in temperature and pressure from 450 to 550 °C and from 3 to 5–7 kbar, respectively, in three metamorphic events is accompanied by a general decrease in the (Fe^{2+} + Mg) $\rightleftharpoons$ Al substitution. Furthermore, the rim of the zoned crystals formed during or after the uplift from an early high pressure to a late medium pressure, as shown by the texture of the beryls, is more rich in Fe^{2+} and Mg than the core. Anyway these ideas need a major investigation with further experimental studies on the behavior of the beryl structure in different pressure and temperature conditi-

tions, but the use of beryl as geobarometer or geothermometer in pegmatitic or metamorphic processes seems possible.

REFERENCES CITED

Aines, R.D., and Rossman, G.R. (1984) The high temperature behavior of water and carbon dioxide in cordierite and beryl. American Mineralogist, 69, 319–327.

Appleman, D.E., and Evans, H.T., Jr. (1963) Job 9214: Indexing and least-squares refinement of powder diffraction data. National Technical Information Service, U.S. Department of Commerce, Springfield, Virginia. Document PB 216-188.

Armbruster, T. (1985) Effect of H_2O on the structure of low cordierite: A single crystal X-ray study. Proceedings of the IMA Meeting 1982, Varna, Bulgaria, in press.

———(1986) Role of Na in the structure of low cordierite: A single-crystal X-ray study. American Mineralogist, 71, 746–757.

Aurisicchio, C., Fioravanti, G.C., and Grubessi, O. (1986) Electron microscopy and X-ray microanalysis evidence for the genesis of the red beryl from Utah (U.S.A.). Proceedings, 11th International Congress on Electron Microscopy, Kyoto, Japan, 2, 1699–1700.

Bakakin, V.V., and Belov, N.V. (1962) Crystal chemistry of beryl. Geokhimiya, 5, 420–433.

Bakakin, V.V., Rilov, G.M., and Belov, N.V. (1969) Crystal structure of a lithium-bearing beryl. Doklady Akademii Nauk SSSR, 188, 659–662.

———(1970) X-ray diffraction data for identification of beryl isomorphs. Geokhimiya, 11, 1302–1311.

Barabanov, V.F. (1980) Geochimie et typomorphisme des aigues-marines zonées. Société Française de Minéralogie et de Cristallographie, Bulletin de Minéralogie, 103, 79–87.

Bariand, P., and Poullin, J.F. (1978) The pegmatites of Lagman, Nuristan, Afghanistan. Mineralogical Record, 9, 301–308.

Bernas, B. (1968) A new method for decomposition and comprehensive analysis by atomic absorption spectrometry. Analytical Chemistry, 40, 1682–1686.

Beus, A.A. (1960) Geochemistry of berillium. Genetic types of beryl deposits. Izdanie Akademii Nauk SSSR, Moscow.

Bragg, W.L., and West, J. (1926) The structure of beryl. Proceedings of the Royal Society London, 3A, 691–714.

Brown, G.E., Jr., and Mills, B.A. (1986) High-temperature structure and crystal chemistry of hydrous alkali-rich beryl from the Harding pegmatite, Taos County, New Mexico. American Mineralogist, 71, 547–556.

Brown, I.D., and Wu, K.K. (1976) Empirical parameters for calculating cation-oxygen bond valences. Acta Crystallographica, 32B, 1957–1959.

Černý, P. (1975) Alkali variations in pegmatitic beryl and their petrogenetic implications. Neues Jahrbuch für Mineralogie Abhandlungen, 123, 198–212.

Černý, P., and Simpson, F.M. (1977) The Tanco pegmatite at Bernic Lake, Manitoba. IX. Beryl. Canadian Mineralogist, 15, 489–499.

Černý, P., and Turnock, A.C. (1975) Beryl from the granitic pegmatites at Greer Lake, southeastern Manitoba. Canadian Mineralogist, 13, 55–61.

Cohen, J.P., Ross, F.K., and Gibbs, G.V. (1977) An X-ray and neutron diffraction study of hydrous low cordierite. American Mineralogist, 62, 67–78.

De Almeida Sampaio Filho, H., Sighinolfi, G., and Galli, E. (1973) Contribution to crystal chemistry of beryl. Contributions to Mineralogy and Petrology, 38, 279–290.

Evans, H.T., Jr., and Mrose, M.E. (1968) Crystal chemical studies of cesium beryl. Geological Society of America Special Paper 101, Abstracts for 1966, 63.

Flamini, A., Gastaldi, L., Grubessi, O., and Viticoli, S. (1983) Risultati preliminari di sintesi di smeraldi. La Gemmologia, Milano, 9, 6–9.

Franz, G., Grundmann, G., and Ackermand, D. (1986) Rock forming beryl from a regional metamorphic terrain (Tauern window, Austria): Parageneses and crystal chemistry. TMPM Tschermaks Mineralogische und Petrographische Mitteilungen, 35, 167–192.

Ganguli, D. (1968) Crystal chemical considerations in beryl. Central Glass and Ceramic Research Institute Bulletin, 15, 6–10.

Ghera, A., and Lucchesi, S. (1987) An unusual vanadium-beryl from Kenia. Neues Jahrbuch für Mineralogie Monatshefte, 263–274.

Gibbs, G.V., Breck, D.W., and Meagher, E.P. (1968) Structural refinement of hydrous and anhydrous synthetic beryl and emerald. $Al_2Be_3Si_6O_{18}$, $Al_{1.9}Cr_{0.1}Be_3Si_6O_{18}$. Lithos, 1, 275–285.

Goldman, D.S., Rossman, G.R., and Parkin, K.M. (1978) Channel constituents in beryl. Physics and Chemistry of Minerals, 3, 225–235.

Gubelin, E.G. (1982) Gemstones of Pakistan: Emerald, ruby and spinel. Gems & Gemology, 18, 140–153.

Hall, A., and Walsh, J.N. (1971) The beryl of the Rosses district, Donegal. Mineralogical Magazine, 38, 328–334.

Hänni, H.A. (1980) Mineralogische und mineralchemische untersuchungen an beryll aus alpinen zerrkluften. Inaugural dissertation. University of Basel, Switzerland.

Hawthorne, F.C., and Černý, P. (1977) The alkali-metal positions in Cs-Li beryl. Canadian Mineralogist, 15, 414–421.

Hazen, R.M., and Finger, L.W. (1982) Comparative crystal chemistry. Wiley, New York.

Hazen, R.M., Au, A.Y., and Finger, L.W. (1986) High-pressure crystal chemistry of beryl ($Be_3Al_2Si_6O_{18}$) and euclase (BeAlSiO$_4$OH). American Mineralogist, 71, 977–984.

Hillebrand, W.F. (1905) Red beryl from Utah. American Journal of Science, 4, 330–331.

Hutchison, R.W., and Claus, R.J. (1956) Pegmatite deposits, Alto Ligonha, Portuguese East Africa. Economic Geology, 51, 757–780.

International tables for X-ray crystallography (1974) Vol. IV. Kynoch Press, Birmingham, England.

Jahns, R.H., and Wright, L.A. (1951) Gem and lithium-bearing pegmatite of the Pala district, San Diego County, California. California Division Mines Special Report, 7-a, 2–72.

Keller, P. (1981) Emeralds of Colombia. Gems & Gemology, 17, 80–92.

Lind, Th., Schmetzer, K., and Bank, H. (1984) Schleifuwurdige blaue und grune berylle (aquamarine und smaragde) aus Nigeria. Zeitschrift der Deutschen Gemmologichen Gesellschaft, 33, 128–138.

Lucchesi, S., and Mairani, A. (1987) Growth formational condition of "three-stage" beryl crystals from Minas Gerais, Brazil. Neues Jahrbuch für Mineralogie, Abhandlungen, 157, 118.

Morosin, B. (1972) Structure and thermal expansion of beryl. Acta Crystallographica, 28, 1899–1903.

Nassau, K., and Wood, D.L. (1968) An examination of red beryl from Utah. American Mineralogist, 53, 801–806.

North, A.C.T., Phillips, D.C., and Mathews, F.S. (1968) A semi-empirical method of absorption correction. Acta Crystallographica, 24A, 351–359.

Polupanova, T.I., Petrov, V.L., Kruzhalov, A.V., Laskovenkov, A.F., and Nikitin, V.S. (1985) The thermal stability of beryl. Geokhimiya, 1, 121–123.

Proctor, K. (1984) Gem pegmatites of Minas Gerais, Brazil: Exploration, occurrence, and aquamarine deposits. Gems & Gemology, 20, 78–100.

Price, D.C., Vance, E.R., Smith, G., Edgar, A., and Dickson, B.L. (1976) Mössbauer effect studies of beryl. Journal de Physique, Colloque C6, Supplement au no. 12, Tome 37, 811–817.

Robinson, K., Gibbs, G.V., and Ribbe, P.H. (1971) Quadratic elongation: A quantitative measure of distortion in coordination polyhedra. Science, 172, 567–570.

Sauer, D.A., (1982) Emeralds from Brazil. International Gemological Symposium, Proceedings, 357–377.

Schaller, W.T., Stevens, R.E., and Jahns, R.H. (1962) An unusual beryl from Arizona. American Mineralogist, 47, 672–699.

Sheldrick, G.M. (1976) SHELX-76, program for crystal structure determination. University of Cambridge, England.

Shigley, J.E., and Foord, E.E. (1985) Gem-quality red beryl from the Wah Wah Mts., Utah. Gem & Gemology, 4, 208–221.

Sinkankas, J. (1981) Emerald and other beryls. Chilton Book Company, Radnor, Pennsylvania, U.S.A., 665 p.

Solovyeva, L.P., and Bakakin, V.V. (1966) Elucidation of the crystalline structure of beryl. Zhurnal Structurnoi Khimii, 7, 469–471.

Staatz, M.H., Griffiths, W.R., and Barnett, P.R. (1965) Differences in the minor elements composition of beryl in various environments. American Mineralogist, 50, 1783–1795.

Tynsdale-Biscoe, R. (1952) The geology of the Bikita tin-field, Southern Rhodesia. Transactions of the Geological Survey of South Africa, 54, 11–23.

Vlasov, K.A., and Kutukova, E.J. (1960) Izumrudnye Kopi (emerald mines). Izdanie Akademii Nauk SSSR, Moscow.

Vorma, A., Sahama, Th., and Haapala, I. (1965) Alkali positions in the beryl structure. Comptes Rendus de la Société Geologique de Finlande, 37, 119–129.

Wood, D., and Nassau, K. (1967) Infrared spectra of foreign molecules in beryl. Journal of Chemical Physics, 47, 2220–2228.

———(1968) The characterization of beryl and emerald by visible and infrared absorption spectroscopy. American Mineralogist, 53, 777–800.

Wallace, J.H., and Wenk, H.R. (1980) Structure variation in low cordierites. American Mineralogist, 65, 96–111.

Zoltai, T. (1960) Classification of silicates and other minerals with tetrahedral structures. American Mineralogist, 45, 960–973.